doi:10.1093/brain/awq091 Brain 2010: 133; 1772–1778 | 1772

BRAIN
A JOURNAL OF NEUROLOGY

In vivo visualization of α-synuclein deposition by carbon-11-labelled 2-[2-(2-dimethylaminothiazol-5-yl)ethenyl]-6-[2-(fluoro)ethoxy]benzoxazole positron emission tomography in multiple system atrophy

Akio Kikuchi,[1] Atsushi Takeda,[1] Nobuyuki Okamura,[2] Manabu Tashiro,[3] Takafumi Hasegawa,[1] Shozo Furumoto,[2,4] Michiko Kobayashi,[1] Naoto Sugeno,[1] Toru Baba,[1] Yasuo Miki,[5] Fumiaki Mori,[5] Koichi Wakabayashi,[5] Yoshihito Funaki,[4] Ren Iwata,[4] Shoki Takahashi,[6] Hiroshi Fukuda,[7] Hiroyuki Arai,[8] Yukitsuka Kudo,[9] Kazuhiko Yanai[2] and Yasuto Itoyama[1]

1 Department of Neurology, Graduate School of Medicine, Tohoku University, Sendai, 980-8574 Japan
2 Department of Pharmacology, Graduate School of Medicine, Tohoku University, Sendai, 980-8575 Japan
3 Division of Cyclotron Nuclear Medicine, Cyclotron and Radioisotope Centre, Tohoku University, Sendai, 980-8578 Japan
4 Division of Radiopharmaceutical Chemistry, Cyclotron and Radioisotope Centre, Tohoku University, Sendai, 980-8578 Japan
5 Department of Neuropathology, Institute of Brain Science, Hirosaki University Graduate School of Medicine, Hirosaki, 036-8562 Japan
6 Department of Diagnostic Radiology, Graduate School of Medicine, Tohoku University, Sendai, 980-8575 Japan
7 Department of Nuclear Medicine and Radiology, Institute of Development, Ageing and Cancer, Tohoku University, Sendai, 980-8575 Japan
8 Department of Geriatric and Respiratory Medicine, Institute of Development, Ageing and Cancer, Tohoku University, Sendai, 980-8575 Japan
9 Innovation of New Biomedical Engineering Centre, Tohoku University, Sendai, 980-8574 Japan

Correspondence to: Atsushi Takeda,
Department of Neurology,
Graduate School of Medicine,
Tohoku University,
1-1 Seiryo-machi,
Aoba-ku, Sendai, Miyagi,
980-8574, Japan
E-mail: atakeda@em.neurol.med.tohoku.ac.jp

The histopathological hallmark of multiple system atrophy is the appearance of intracellular inclusion bodies, named glial cytoplasmic inclusions, which are mainly composed of α-synuclein fibrils. *In vivo* visualization of α-synuclein deposition should be used for the diagnosis and assessment of therapy and severity of pathological progression in multiple system atrophy. Because 2-[2-(2-dimethylaminothiazol-5-yl)ethenyl]-6-[2-(fluoro)ethoxy] benzoxazole could stain α-synuclein-containing glial cytoplasmic inclusions in post-mortem brains, we compared the carbon-11-labelled 2-[2-(2-dimethylaminothiazol-5-yl)ethenyl]-6-[2-(fluoro)ethoxy] benzoxazole positron emission tomography findings of eight multiple system atrophy cases to those of age-matched normal controls. The positron emission tomography data demonstrated high distribution volumes in the subcortical white matter (uncorrected $P<0.001$), putamen and posterior cingulate cortex (uncorrected $P<0.005$), globus pallidus, primary motor cortex and anterior cingulate cortex (uncorrected $P<0.01$), and substantia nigra (uncorrected $P<0.05$) in multiple system atrophy cases compared to the normal controls. They were coincident with glial cytoplasmic inclusion-rich brain areas in

Received January 13, 2010. Revised March 15, 2010. Accepted March 17, 2010. Advance Access publication April 29, 2010

multiple system atrophy and thus, carbon-11-labelled 2-[2-(2-dimethylaminothiazol-5-yl)ethenyl]-6-[2-(fluoro)ethoxy] benzoxazole positron emission tomography is a promising surrogate marker for monitoring intracellular α-synuclein deposition in living brains.

Keywords: glial cytoplasmic inclusion; Lewy body; β-amyloid; Parkinson's disease; Pittsburgh compound B

Abbreviations: BF-227 = 2-[2-(2-dimethylaminothiazol-5-yl)ethenyl]-6-[2-(fluoro)ethoxy]benzoxazole; MSA = multiple system atrophy; PIB = Pittsburgh compound B

Introduction

Multiple system atrophy (MSA) is a sporadic, progressive neurodegenerative disease characterized by variable severity of parkinsonism, cerebellar ataxia, autonomic failure and pyramidal signs. Although MSA was originally described as three separate diseases [olivopontocerebellar atrophy (Dejerine and Thomas, 1900), striatonigral degeneration (van der Eecken *et al.*, 1960) and Shy–Drager syndrome (Shy and Drager, 1960)], they are currently classified into a single disease that consists of MSA with predominant parkinsonism and MSA with predominant cerebellar ataxia (Gilman *et al.*, 1999). The histopathological hallmark of MSA, glial cytoplasmic inclusions, comprises mainly insoluble fibrils of phosphorylated α-synuclein (Wakabayashi *et al.*, 1998). Thus, it is suggested that the MSA is in the family of α-synucleinopathies (Marti *et al.*, 2003) including Parkinson's disease and dementia with Lewy bodies, which are characterized by the presence of Lewy bodies, representing other brain inclusions composed of α-synuclein.

Previous neuropathological studies indicated that the appearance of glial cytoplasmic inclusions preceded the clinical onset of MSA (Fujishiro *et al.*, 2008) and the amount of α-synuclein deposition correlated with the disease progression (Wakabayashi and Takahashi, 2006). Therefore, it is plausible that the formation of α-synuclein deposits plays a key role in neurodegeneration, and that compounds that inhibit this process may be therapeutically useful for MSA and other α-synucleinopathies. In fact some compounds, including antioxidants (Ono and Yamada, 2006) and non-steroidal anti-inflammatory drugs (Hirohata *et al.*, 2008), were reported to have potent anti-fibrillogenic and fibril-destabilizing effects on aggregated α-synucleins, and received much attention as possible new therapeutic agents (Ono and Yamada, 2006; Hirohata *et al.*, 2008). Detection of α-synuclein deposition *in vivo* could theoretically allow early diagnosis even at the presymptomatic stage, as well as assess disease progression and possible therapeutic effects in the living brain of patients with MSA.

Although Pittsburgh compound B (PIB) and other compounds were reported to be useful in detecting senile plaques *in vivo*, to our knowledge, there were no imaging probes currently available for *in vivo* detection of α-synuclein deposition. Recently, 2-[2-(2-dimethylaminothiazol-5-yl)ethenyl]-6-[2-(fluoro)ethoxy] benzoxazole (BF-227), known as a positron emission tomography (PET) probe for *in vivo* detection of dense β-amyloid deposits in humans (Kudo *et al.*, 2007), was reported to bind with synthetic α-synuclein aggregates as well as β-amyloid fibrils *in vitro* (Fodero-Tavoletti *et al.*, 2009). In the present study, we demonstrated that BF-227 could stain α-synuclein-containing glial cytoplasmic inclusions in post-mortem tissues and moreover, that a PET study with carbon-11-labelled BF-227 ([11C]-BF-227) could detect α-synuclein deposits in the living brains of patients with MSA.

Materials and methods

Neuropathological staining

Brain specimens

The subjects of the first part of the study were nine autopsy cases, including three with Parkinson's disease, three with dementia with Lewy bodies and three with MSA. The above diagnoses were confirmed both clinically and histopathologically. Brain tissues taken from the temporal cortex and substantia nigra of patients with Parkinson's disease and dementia with Lewy bodies, and pontine base of patients with MSA, were fixed in 20% buffered formalin for 72 h at 4°C, and vibratome sections (50 μm thick) were prepared.

Fluorescence and immunohistochemical analysis

BF-227 was dissolved in 50% ethanol containing 5% polysorbate (Tween 80; Wako, Osaka, Japan). The sections were slide mounted, incubated in 100 μM BF-227 for 30 min, dipped three times in phosphate buffer, and coverslipped with non-fluorescent mounting medium (Vectashield, Vector Laboratories, Burlingame, CA, USA). Fluorescence images were visualized using an Olympus Provis fluorescence microscope (Olympus, Tokyo, Japan) at wavelength 400 nm. After photographing fluorescent structures, BF-227-labelled sections were immunostained with primary antibodies against phosphorylated α-synuclein (#64; Wako). For phosphorylated α-synuclein immunohistochemistry, the sections were pre-treated with 99% formic acid for 5 min, then incubated overnight at 4°C with each primary antibody followed by incubation with the biotinylated secondary antibodies and the avidin–biotin–peroxidase complex (Vectastain ABC kit, Vector Laboratories). Diaminobenzidine was used as the chromogen.

PET study

Subjects

Eight patients with probable MSA and eight age-matched normal subjects were studied to examine the distribution of [11C]-BF-227 in the brain. All probable MSA patients were diagnosed on the second consensus criteria for probable MSA (Gilman *et al.*, 2008). Table 1 summarizes the clinical features of these patients. There were no significant differences in age, disease duration and unified MSA rating scale score between the MSA with predominant parkinsonism

Table 1 Subject profile

	Normal controls	MSA		
		Total	MSA-P	MSA-C
n	8	8	4	4
Gender (F/M)	4/4	4/4	1/3	3/1
Age (years)	64.3 ± 5.90	57.4 ± 10.1	60.5 ± 11.1	54.3 ± 9.50
Duration (years)		1.50 ± 0.54	1.75 ± 0.50	1.25 ± 0.50
UMSARS score		36.1 ± 8.87	41.5 ± 9.39	30.8 ± 4.27

Data are mean ± SD.
MSA-P = MSA with predominant parkinsonism; MSA-C = MSA with predominant cerebellar ataxia; UMSARS = unified MSA rating scale.

subgroup and the MSA with predominant cerebellar ataxia subgroup. The normal control group comprised volunteers without impairment of cognitive and motor functions who had no cerebrovascular lesions on magnetic resonance imaging. The study protocol was approved by the Ethical Committee of Tohoku University Graduate School of Medicine, and a written informed consent was obtained from each subject after being given a complete description of the study.

Radiosynthesis of [^{11}C]-BF-227

BF-227 and its N-desmethylated derivative (a precursor of [^{11}C]-BF-227) were custom-synthesized by Tanabe R&D Service Co. (Tokyo) (Kudo *et al.*, 2007). [^{11}C]-BF-227 was synthesized from the precursor by N-methylation in dimethyl sulphoxide using [^{11}C]-methyl triflate (Jewett, 1992; Iwata *et al.*, 2001). After quenching the reaction with 5% acetic acid in ethanol, [^{11}C]-BF-227 was separated from the crude mixture by semi-preparative reversed-phase high-performance liquid chromatography and then isolated from the collected fraction by solid-phase extraction. The purified [^{11}C]-BF-227 was solubilized in isotonic saline containing 1% polysobate-80 and 5% ascorbic acid. The saline solution was filter sterilized with a 0.22 mm Millipore® filter for clinical use. The radiochemical yields were >50% based on [^{11}C]-methyl triflate, and the specific radioactivities were 119–138 GBq/mmol at the end of synthesis. The radiochemical purities were >95%.

PET procedure

The [^{11}C]-BF-227 PET study was performed using a SET-2400W PET scanner (Shimadzu Inc., Japan) under resting condition with eyes closed in a dark room. Following a 68Ge/Ga transmission scan of 300–400 s duration, an emission scan was started soon after intravenous injection of 3.7–8.3 mCi of [^{11}C]-BF-227. A dynamic series of PET scans were acquired over 60 min with 23 frames. Emission data were corrected for attenuation, dead time and radioactive decay. Standardized uptake value images were obtained by normalizing tissue concentration by the injected dose and body mass. Arterial blood samples (1.5 ml) from the radial or brachial artery were collected from each subject at 10 s intervals for the first 2 min, and subsequently at intervals increasing progressively from 1 to 10 min until 60 min after the injection of [^{11}C]-BF-227 except for one subject, from whom arterialized venous blood samples (1.5 ml) from a hand vein heated in a far-infrared mat were collected at the same time intervals. The plasma obtained by centrifugation at 3000*g* for 3 min was weighed and the radioactivity was measured with a well-type scintillation counter. Additional arterial blood samples were obtained at four time points during the study (5, 15, 30 and 60 min) for the determination of radiolabelled metabolites in plasma using high-performance liquid chromatography. These data yielded values of the unchanged fraction of parent radiotracer throughout the time frame of the study. A multi-exponential equation was used to describe this curve and to estimate the parent fraction at each measured plasma curve time point.

PET image analysis

To measure α-synuclein deposition densities in the brain, the distribution volume, the ratio of [^{11}C]-BF-227 concentration in tissue to that in plasma at equilibrium, was calculated by Logan's graphical analysis (Logan, 2000), since BF-227 reversibly binds to α-synuclein depositions (Tashiro *et al.*, 2009). Region of interest analysis was performed to evaluate the regional distribution of [^{11}C]-BF-227. Circular regions of interest were placed on individual axial PET images in the frontal cortex, primary motor cortex, parietal cortex, medial temporal cortex, lateral temporal cortex, occipital cortex, anterior cingulate cortex, posterior cingulate cortex, subcortical white matter, caudate nucleus, putamen, globus pallidus, thalamus, substantia nigra, midbrain tegmentum, pons and cerebellar cortex, referring to the individual magnetic resonance images.

Statistical analysis

Data were expressed as mean ± SD. Differences in distribution volume between normal control and MSA groups were evaluated by one-way analysis of variance followed by Bonferroni's multiple comparison test (GraphPad Prism Software).

Results

Neuropathological staining

In the post-mortem brains with Parkinson's disease, double-labelling immunostaining with BF-227 fluorostaining and anti-phosphorylated α-synuclein antibody demonstrated co-localization of the proteins in Lewy bodies in the substantia nigra (Fig. 1A and B). Strong BF-227 staining was observed in the central core (Fig. 1A). BF-227 was also detected in the cortical Lewy bodies in dementia with Lewy bodies (Fig. 1C and D). In MSA, double-labelling experiments using BF-227 and anti-phosphorylated α-synuclein antibody demonstrated BF-227 fluorescent signal in the most of glial cytoplasmic inclusions in the pontine base (Fig. 1E and F).

PET study

Tissue time activity curves of [^{11}C]-BF-227 in the brain indicated more gradual clearance from the brain in patients with MSA compared with normal subjects following initial rapid uptake of radioactivity (Fig. 2A). Relatively high concentrations of [^{11}C]-BF-227 radioactivity were observed in the subcortical white matter and lenticular nucleus in MSA, in which relatively intense α-synuclein deposits were found in the post-mortem brain (Fig. 2B). [^{11}C]-BF-227 exhibited linear regression curves on Logan plot analysis in all brain regions examined. Since the slopes of the regression lines represent the distribution volume of the tracer, these findings indicated a higher distribution volume of [^{11}C]-BF-227 in MSA than in normal controls (Fig. 2C). The regional distribution volume values were high in the subcortical white matter (uncorrected $P < 0.001$), putamen and posterior cingulate cortex

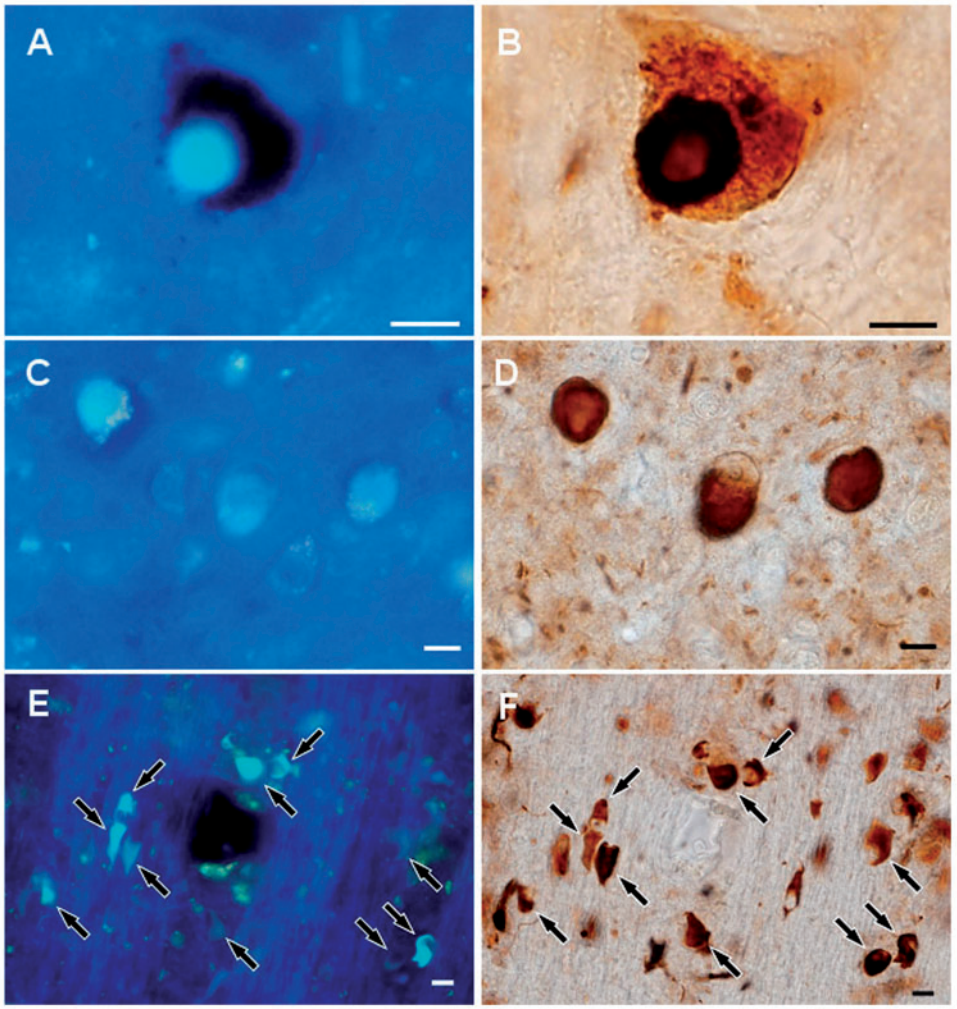

Figure 1 Neuropathological findings of BF-227 fluorostaining and anti-phosphorylated α-synuclein antibody immunostaining. BF-227 fluorostaining (**A** and **C**) and anti-phosphorylated α-synuclein antibody immunostaining (**B** and **D**) showed colocalization of these proteins in brainstem-type Lewy bodies in the substantia nigra of patients with Parkinson's disease (**A** and **B**) and in cortical Lewy bodies in the temporal lobe of patients dementia with Lewy bodies (**C** and **D**). Similarly, BF-227 fluorostaining (**E**) and anti-phosphorylated α-synuclein antibody immunostaining (**F**) were codetected in glial cytoplasmic inclusions in the pontine base of a patient with MSA. BF-227 histofluorescence was observed in the most of glial cytoplasmic inclusions (arrows). Bars = 10 μm.

(uncorrected $P<0.005$), globus pallidus, primary motor cortex and anterior cingulate cortex (uncorrected $P<0.01$) and substantia nigra (uncorrected $P<0.05$) in patients with MSA compared to the normal controls (Table 2 and Fig. 2D). It is noteworthy that the distribution volume of [11C]-BF-227 was significantly high in the subcortical white matter even if Bonferroni's multiple comparison test was applied. On the other hand, no obvious differences were found in either the distribution or degree of binding between the MSA with predominant parkinsonism and MSA with predominant cerebellar ataxia subgroups.

Discussion

The BF-227 stained α-synuclein-containing Lewy bodies (Fig. 1A–D) and glial cytoplasmic inclusions (Fig. 1E and F) in formalin-fixed tissue sections as well as β-amyloid-containing senile plaques in paraffin-embedded tissue sections (Kudo *et al.*, 2007). These results were consistent with the previous findings showing BF-227 binding to synthetic α-synuclein fibrils with high affinity (K_d 9.63 nM) (Fodero-Tavoletti *et al.*, 2009), and to Lewy bodies in paraffin-embedded tissue sections (Fodero-Tavoletti *et al.*, 2009).

The anti-phosphorylated α-synuclein antibody immunostained the halo region more intensively compared with the central core in Lewy bodies in the substantia nigra of Parkinson's disease, while the BF-227 staining was intensely observed in the core of Lewy bodies (Fig. 1A and B). Because intense thioflavin S staining was also reported in the core of nigral Lewy bodies (Duda *et al.*, 2000), the core is thought to be rich in β-sheet structures. Similar to thioflavin S, the BF-227 staining is considered to recognize amyloid-like β-pleated sheets, and it was suggested to be the reason for the more intense BF-227 staining in the core of Lewy bodies. In addition, the high density of the core structure

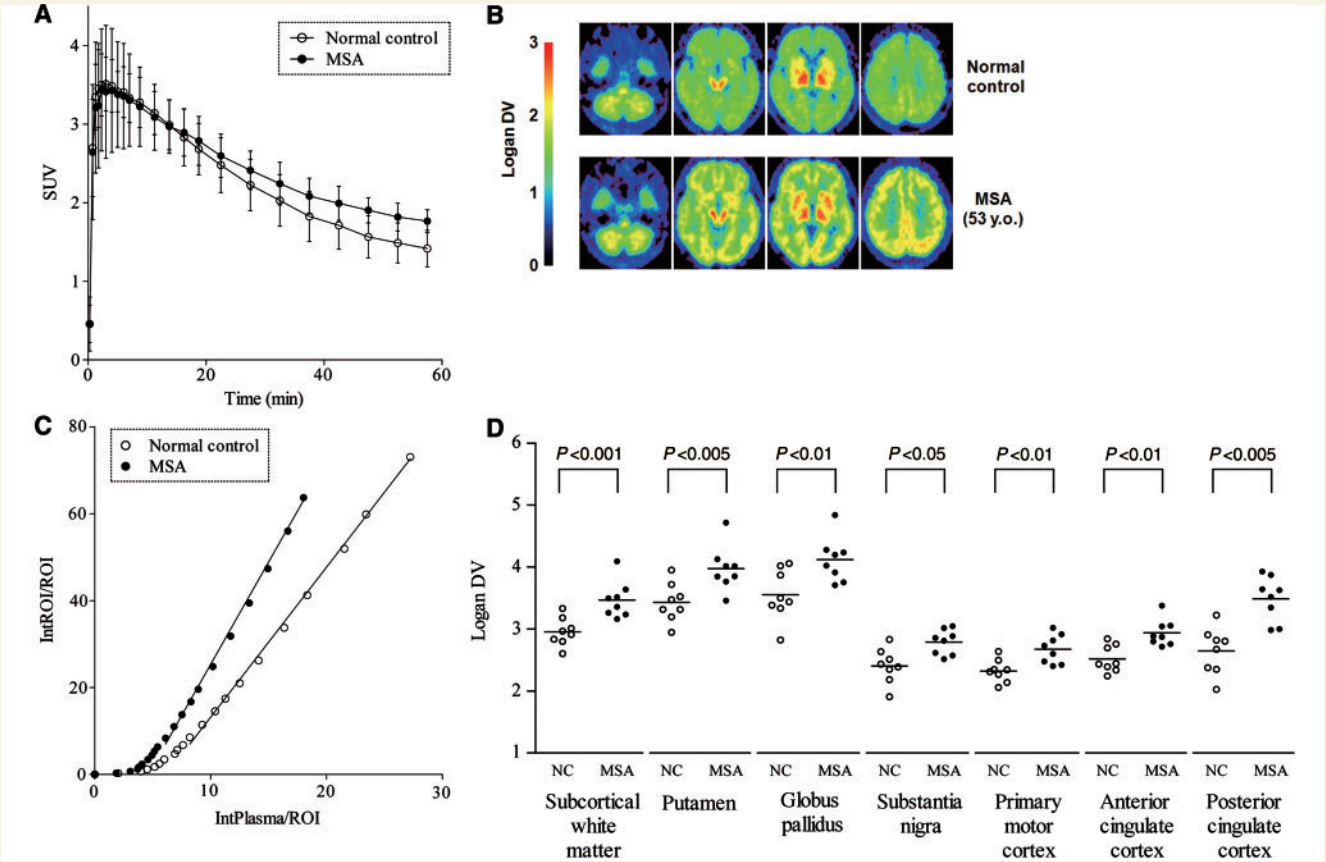

Figure 2 [^{11}C]-BF-227 PET findings in MSA. Time activity curves showed initial rapid uptake of radioactivity followed by gradual clearance in the putamen of both normal subjects and MSA cases. Data are mean ± SD of eight normal subjects and eight patients with MSA (**A**). In a representative patient with MSA with predominant cerebellar ataxia, the regional distribution volumes were mapped to the subcortical white matter and lentiform nucleus compared to normal control (**B**). Typical Logan plots for the putamen were presented in a representative patient with MSA with predominant cerebellar ataxia and a normal control. The slopes of the linear regression curves on Logan plot analysis represent the distribution volume of the tracer in the putamen (**C**). There were differences in the mean regional distribution volume values between patients with MSA and normal control in the subcortical white matter (uncorrected $P < 0.001$), putamen and posterior cingulate cortex (uncorrected $P < 0.005$), globus pallidus, primary motor cortex and anterior cingulate cortex (uncorrected $P < 0.01$) and substantia nigra (uncorrected $P < 0.05$). Data of individual subjects (symbols) and mean values (horizontal lines) (**D**). SUV = standardized uptake value; DV = distribution volume; ROI = region of interest.

may often prevent the penetration of antibodies into this region (Galloway *et al.*, 1992), since electron microscopic studies revealed that vesicular structures were tightly packed in the core of Lewy bodies (Takahashi and Wakabayashi, 2005). On the other hand, not all glial cytoplasmic inclusions stained by anti-phosphorylated α-synuclein antibody were always positive for BF-227 staining (Fig. 1E and F). In the process of oligodendroglial pathology, it was believed that α-synuclein deposits as amorphous state and then forms fibrillar structures (Gai *et al.*, 2003; Stefanova *et al.*, 2005). In fact, part of glial cytoplasmic inclusions were reported to be α-synuclein-negative (Sakamoto *et al.*, 2005) and therefore, it seems reasonable that some of glial cytoplasmic inclusions were not composed of β-sheet fibrils and were negative for BF-227 staining.

The regional distribution volume of [^{11}C]-BF-227 was the highest in the subcortical white matter, followed by the putamen, posterior cingulate cortex, anterior cingulate cortex, globus pallidus, primary motor cortex and substantia nigra, in which glial cytoplasmic inclusions were densely distributed (Papp and Lantos, 1994; Inoue *et al.*, 1997; Wakabayashi and Takahashi, 2006) and large increases of α-synuclein content were found (Tong *et al.*, 2010) in the post-mortem brains. Thus, it was suggested that the distributions of [^{11}C]-BF-227 could properly reflect those of the α-synuclein deposits *in vivo*. On the other hand, the regional distribution volume in other affected brain regions, such as the cerebellum and pons (Ozawa *et al.*, 2004; Wakabayashi and Takahashi, 2006), did not show higher values relative to the normal control group. The glial cytoplasmic inclusions in cerebellum were reported to decrease along with the disease progression and concomitant neuronal loss (Inoue *et al.*, 1997). Therefore, it is plausible that the accumulation levels of glial cytoplasmic inclusions are changing and do not always increase with the disease progression (Mochizuki *et al.*, 1992; Inoue *et al.*, 1997). Moreover, due to the remarkable cerebellar and pontine atrophy,

Table 2 Distribution volume of [11C]BF-227

	Normal controls	MSA
Frontal cortex	2.28 ± 0.18	2.46 ± 0.22
Primary motor cortex	2.40 ± 0.28	2.79 ± 0.20¶
Parietal cortex	2.48 ± 0.26	2.63 ± 0.24
Medial temporal cortex	2.44 ± 0.21	2.82 ± 0.31
Lateral temporal cortex	2.42 ± 0.19	2.63 ± 0.23
Occipital cortex	2.43 ± 0.20	2.72 ± 0.27
Anterior cingulate cortex	2.32 ± 0.18	2.67 ± 0.23¶
Posterior cingulate cortex	2.52 ± 0.22	2.94 ± 0.22†
Subcortical white matter	2.65 ± 0.38	3.49 ± 0.36‡
Caudate nucleus	2.70 ± 0.21	3.05 ± 0.34
Putamen	2.95 ± 0.23	3.47 ± 0.30†
Globus pallidus	3.43 ± 0.31	3.97 ± 0.36¶
Thalamus	3.50 ± 0.28	4.03 ± 0.31
Substantia nigra	3.55 ± 0.41	4.12 ± 0.36*
Midbrain tegmentum	3.53 ± 0.54	3.45 ± 0.47
Pons	3.63 ± 0.54	3.88 ± 0.42
Cerebellar cortex	2.32 ± 0.22	2.16 ± 0.29

Data are mean ± SD.
*Uncorrected $P < 0.05$.
¶Uncorrected $P < 0.01$.
†Uncorrected $P < 0.005$.
‡Uncorrected $P < 0.001$.

the distribution volume in these regions might be underestimated. Correction for partial volume loss is therefore needed to improve the accuracy of quantification in the cerebellum and brainstem of MSA. BF-227 fluorescent signal was detected in β-amyloid plaques as well as glial cytoplasmic inclusions and Lewy bodies (Fig. 1A–F) in neuropathological staining (Kudo *et al.*, 2007). However, the differences in the distribution of [11C]-BF-227 by PET could discriminate MSA from Alzheimer's disease, which showed high distribution of [11C]-BF-227 in the temporoparietal–occipital region (Kudo *et al.*, 2007). In our preliminary studies, Parkinson's disease and dementia with Lewy bodies also showed quite different patterns of distribution volumes from those of MSA (data not shown). Therefore, MSA could be distinguished from other degenerative diseases such as Alzheimer's disease, Parkinson's disease and dementia with Lewy bodies by the [11C]-BF-227 PET.

The affinity of BF-227 to α-synuclein fibrils (K_d 9.63 nM) was reported to be almost identical to that of PIB (K_d 10.07 nM) (Fodero-Tavoletti *et al.*, 2007, 2009). However, in the post-mortem human brain, the PIB binding was not colocalized with α-synuclein-positive Lewy bodies in two reports (Fodero-Tavoletti *et al.*, 2007; Ye *et al.*, 2008) although one report showed PIB binding to Lewy bodies in the substantia nigra of Parkinson's disease (Maetzler *et al.*, 2008). Therefore, there is controversy as to whether PIB binds to α-synuclein-containing Lewy bodies. Moreover, there have been no reports showing that PIB could detect α-synuclein deposits in α-synucleinopathies by PET (Fodero-Tavoletti *et al.*, 2007; Johansson *et al.*, 2008; Maetzler *et al.*, 2008). The hydroxy group in PIB (Mathis *et al.*, 2003) may prevent it from passing through the cell membranes and thereby detecting α-synuclein depositions in the cytoplasm, however, the BF-227 is more lipophilic than PIB (Mathis *et al.*, 2003), and may easily pass into the cytoplasm and bind to α-synuclein aggregates. As shown in the present study, BF-227 is a promising tracer to detect glial cytoplasmic inclusions. Further studies are warranted to verify whether Lewy bodies in other α-synucleinopathies as well as glial cytoplasmic inclusions can be detected by [11C]-BF-227 PET.

In conclusion, the BF-227 could bind to α-synuclein-containing glial cytoplasmic inclusions (Fig. 1E and F) in the post-mortem brain, and the [11C]-BF-227 PET demonstrated high signals in the glial cytoplasmic inclusion-rich brain regions including subcortical white matter, putamen, globus pallidus, primary motor cortex and anterior and posterior cingulate cortex (Table 2 and Fig. 2D). These results suggest that [11C]-BF-227 PET is a suitable surrogate maker for monitoring α-synuclein deposits in living brains with MSA and could be a potential tool to monitor the effectiveness of neuroprotective therapy for α-synucleinopathies.

Funding

Grant for 'the Research Committee for Ataxic Diseases' of the Research on Measures for Intractable Diseases from the Ministry of Health, Labour and Welfare, Japan (partial).

References

Dejerine J, Thomas A. L'atrophie olivo-ponto-cérébelleuse. Nouvelle Iconographie Salpêtrière 1900; 13: 330–7.

Duda JE, Lee VM, Trojanowski JQ. Neuropathology of synuclein aggregates. J Neurosci Res 2000; 61: 121–7.

Fodero-Tavoletti MT, Mulligan RS, Okamura N, Furumoto S, Rowe CC, Kudo Y, et al. In vitro characterisation of BF227 binding to alpha-synuclein/Lewy bodies. Eur J Pharmacol 2009; 617: 54–8.

Fodero-Tavoletti MT, Smith DP, McLean CA, Adlard PA, Barnham KJ, Foster LE, et al. In vitro characterization of Pittsburgh compound-B binding to Lewy bodies. J Neurosci 2007; 27: 10365–71.

Fujishiro H, Ahn TB, Frigerio R, DelleDonne A, Josephs KA, Parisi JE, et al. Glial cytoplasmic inclusions in neurologically normal elderly: prodromal multiple system atrophy? Acta Neuropathol 2008; 116: 269–75.

Gai WP, Pountney DL, Power JH, Li QX, Culvenor JG, McLean CA, et al. alpha-Synuclein fibrils constitute the central core of oligodendroglial inclusion filaments in multiple system atrophy. Exp Neurol 2003; 181: 68–78.

Galloway PG, Mulvihill P, Perry G. Filaments of Lewy bodies contain insoluble cytoskeletal elements. Am J Pathol 1992; 140: 809–22.

Gilman S, Low PA, Quinn N, Albanese A, Ben-Shlomo Y, Fowler CJ, et al. Consensus statement on the diagnosis of multiple system atrophy. J Neurol Sci 1999; 163: 94–8.

Gilman S, Wenning GK, Low PA, Brooks DJ, Mathias CJ, Trojanowski JQ, et al. Second consensus statement on the diagnosis of multiple system atrophy. Neurology 2008; 71: 670–6.

Hirohata M, Ono K, Morinaga A, Yamada M. Non-steroidal anti-inflammatory drugs have potent anti-fibrillogenic and fibril-destabilizing effects for alpha-synuclein fibrils in vitro. Neuropharmacology 2008; 54: 620–7.

Inoue M, Yagishita S, Ryo M, Hasegawa K, Amano N, Matsushita M. The distribution and dynamic density of oligodendroglial cytoplasmic inclusions (GCIs) in multiple system atrophy: a correlation between the density of GCIs and the degree of involvement of striatonigral and olivopontocerebellar systems. Acta Neuropathol 1997; 93: 585–91.

Iwata R, Pascali C, Bogni A, Miyake Y, Yanai K, Ido T. A simple loop method for the automated preparation of (11C)raclopride from (11C)methyl triflate. Appl Radiat Isot 2001; 55: 17–22.

Jewett DM. A simple synthesis of [11C]methyl triflate. Int J Rad Appl Instrum [A] 1992; 43: 1383–5.

Johansson A, Savitcheva I, Forsberg A, Engler H, Langstrom B, Nordberg A, et al. [(11)C]-PIB imaging in patients with Parkinson's disease: preliminary results. Parkinsonism Relat Disord 2008; 14: 345–7.

Kudo Y, Okamura N, Furumoto S, Tashiro M, Furukawa K, Maruyama M, et al. 2-(2-[2-Dimethylaminothiazol-5-yl]ethenyl)-6-(2-[fluoro]ethoxy)benzoxazole: a novel PET agent for in vivo detection of dense amyloid plaques in Alzheimer's disease patients. J Nucl Med 2007; 48: 553–61.

Logan J. Graphical analysis of PET data applied to reversible and irreversible tracers. Nucl Med Biol 2000; 27: 661–70.

Maetzler W, Reimold M, Liepelt I, Solbach C, Leyhe T, Schweitzer K, et al. [11C]PIB binding in Parkinson's disease dementia. Neuroimage 2008; 39: 1027–33.

Marti MJ, Tolosa E, Campdelacreu J. Clinical overview of the synucleinopathies. Mov Disord 2003; 18(Suppl): S21–7.

Mathis CA, Wang Y, Holt DP, Huang GF, Debnath ML, Klunk WE. Synthesis and evaluation of 11C-labeled 6-substituted 2-arylbenzothiazoles as amyloid imaging agents. J Med Chem 2003; 46: 2740–54.

Mochizuki A, Mizusawa H, Ohkoshi N, Yoshizawa K, Komatsuzaki Y, Inoue K, et al. Argentophilic intracytoplasmic inclusions in multiple system atrophy. J Neurol 1992; 239: 311–6.

Ono K, Yamada M. Antioxidant compounds have potent anti-fibrillogenic and fibril-destabilizing effects for alpha-synuclein fibrils in vitro. J Neurochem 2006; 97: 105–15.

Ozawa T, Paviour D, Quinn NP, Josephs KA, Sangha H, Kilford L, et al. The spectrum of pathological involvement of the striatonigral and olivopontocerebellar systems in multiple system atrophy: clinicopathological correlations. Brain 2004; 127: 2657–71.

Papp MI, Lantos PL. The distribution of oligodendroglial inclusions in multiple system atrophy and its relevance to clinical symptomatology. Brain 1994; 117(Pt 2): 235–43.

Sakamoto M, Uchihara T, Nakamura A, Mizutani T, Mizusawa H. Progressive accumulation of ubiquitin and disappearance of alpha-synuclein epitope in multiple system atrophy-associated glial cytoplasmic inclusions: triple fluorescence study combined with Gallyas-Braak method. Acta Neuropathol 2005; 110: 417–25.

Shy GM, Drager GA. A neurological syndrome associated with orthostatic hypotension: a clinical-pathologic study. Arch Neurol 1960; 2: 511–27.

Stefanova N, Reindl M, Neumann M, Haass C, Poewe W, Kahle PJ, et al. Oxidative stress in transgenic mice with oligodendroglial alpha-synuclein overexpression replicates the characteristic neuropathology of multiple system atrophy. Am J Pathol 2005; 166: 869–76.

Takahashi H, Wakabayashi K. Controversy: is Parkinson's disease a single disease entity? Yes. Parkinsonism Relat Disord 2005; 11(Suppl 1): S31–7.

Tashiro M, Okamura N, Furumoto S, Kumagai K, Furukawa K, Sugi K, et al. Quantitative analysis of amyloid deposition in Alzheimer's disease patients and healthy volunteers using PET and [11C]BF-227. In: Proceedings of the International Symposium on Early Detection and Rehabilitation Technology of Dementia 2009 (DRD2009). Okayama, Japan, 2009.110–1.

Tong J, Wong H, Guttman M, Ang LC, Forno LS, Shimadzu M, et al. Brain alpha-synuclein accumulation in multiple system atrophy, Parkinson's disease and progressive supranuclear palsy: a comparative investigation. Brain 2010; 133: 172–88.

van der Eecken H, Adams RD, van Bogaert L. Striopallidal-nigral degeneration. An hitherto undescribed lesion in paralysis agitans. J Neuropathol Exp Neurol 1960; 19: 159–61.

Wakabayashi K, Takahashi H. Cellular pathology in multiple system atrophy. Neuropathology 2006; 26: 338–45.

Wakabayashi K, Yoshimoto M, Tsuji S, Takahashi H. Alpha-synuclein immunoreactivity in glial cytoplasmic inclusions in multiple system atrophy. Neurosci Lett 1998; 249: 180–2.

Ye L, Velasco A, Fraser G, Beach TG, Sue L, Osredkar T, et al. In vitro high affinity alpha-synuclein binding sites for the amyloid imaging agent PIB are not matched by binding to Lewy bodies in postmortem human brain. J Neurochem 2008; 105: 1428–37.